J. Nig. Ass. Math. Phys.
Vol. 5 (2001)

ELECTRONIC BAND STRUCTURE OF SOLID C_{60}

F. MATTHEW-OJELABI
Department of Physics, University of Ado-Ekiti, Nigeria

and

J.O.A. IDIODI
Department of Physics, University of Benin, Benin City, Nigeria

ABSTRACT

We present a group theoretical method for the construction of the molecular orbitals of carbon 60 (C_{60}) using 60 atomic orbitals (AO's) per C_{60} molecule. The geometry of the crystalline fcc solid C_{60} and the hypothetical unidirectional structure with space group $Fm\bar{3}$ are adopted in our study. The goal is to provide all the relevant transformation matrices that are required by group theory. These are then used to obtain analytical expressions for the molecular orbitals (MO's) in a form suitable for further calculations. We limit our derivations to the lowest unoccupied molecular orbitals (LUMO's) i.e. the levels relevant to superconductivity in the doped compounds. In a preliminary calculation, the MO's are used to diagonalize a single particle Hamiltonian in a band structure calculation.

1. INTRODUCTION

The football-shaped C_{60} molecule was first synthesized in 1985 [1]. The molecule contains 60 carbon atoms which sit at the 60 vertices of the 20 hexagonal and 12 pentagonal faces of a truncated icosahedron. Each carbon atom of the molecule is bonded to its three neighbour atoms in two different ways: a double bond of length $1.40\,\mathring{A}$ shared by two hexagons, and two single bonds of length $1.46\,\mathring{A}$ shared by a hexagon and a pentagon. The molecule has a diameter of about $7.0\,\mathring{A}$.

Pure solid C_{60} (fullerene) is an organic molecular crystal in which the icosahedral C_{60} molecules occupy the lattice sites of a fcc lattice [2,3] with lattice constant $a = 14.10\,\mathring{A}$. The interactions between the molecules in the solid state are weak and believed to be predominantly of Van der Waals type. Infact, the centres of neighbouring molecules are separated by a distance of about $10\,\mathring{A}$. Solid C_{60} contains two tetrahedral sites and an Octahedral site per molecule or unit cell. These interstitial spaces permit the insertion of metal toms between the C_{60} molecules.

Solid C_{60} can be made to superconduct by alkali-metal doping. The composition A_3C_{60} (with $A_3 = K_3$, K_2Rb, Rb_2K, Rb_3, Rb_2C_s, etc) has been established and known to crystallize in fcc lattice structure [4]. A doping level A_XC_{60} where $X > 3$

will force the structure to change from fcc to bcc or bct and superconductivity disappears. The experimental success in synthesizing macroscopic quantities of solid C_{60} and the discovery of superconductivity in its doped or alloy compounds have spurred great interest in the structural and electronic properties of the C_{60} molecule and also solid C_{60}. The electronic structure is usually one of the starting points in the construction of an appropriate Hamiltonian for the C_{60} system. The Hamiltonian is vital for various theoretical studies.

The electronic band structure of C_{60} has been treated by various workers and the literature on C_{60} is quite vast. A lot of the current effort is directed towards providing simplification to the diverse existing theoretical methods. For instance, in the work by Tit and Kumar [5] four orbitals per carbon atom (i.e. 240 orbitals per molecule) are used to diagonalize a one-electron, tight-binding Hamiltonian in a local density approximation (LDA) type of calculation. The large dimension of their Hamilltonian matrix (240N x 240N) coupled with heavy computational cost warranted the need for simpler methods.

In this paper, we present a preliminary report of a group theoretical method which we have used to determine the electronic band structure of solid C_{60}. The method involves the use of one orbital per carbon atom. Our approach is anchored on the high symmetry (icosahedral) possessed by the C_{60} molecule which allows the derivation of the degenerate MO's analytically. The expected dimension of our Hamiltonian matrix , 60N X 60N, is hugely reduced by symmetry to 3N x 3N which is clearly easier to handle. We consider specifically a unidirectional structural order where N = 1 and as a first step we construct, in section 2 of this work the relevant matrices and molecular orbitals required by the group theory of the problem. The construction of the 3N Bloch sums and the evaluation of the corresponding elements of the single-particle tight-binding Hamiltonian together with the electronic band structure and the density of states (DOS) then follow in subsequent sections.

This work differs in approach from the recent work of Lin and Nori [6] who employ analytically the recursion and moment methods to determine the electronic structure of C_{60}. Our work is similar in spirit however to the work of Laouini et al [7] where the usage of group theory as discussed in the standard text of Cotton [8], is employed to bring about tremendous simplification to the band structure problem.

Despite the vast amount of work already published on the C_{60} system, the 3 x 3 matrix representations for the 120 symmetry elements of the C_{60} molecule are difficult to find in the literature. Since a knowledge of these matrices is crucial in the approach adopted in this work, the construction and full listing of these matrices is partly the motivation for this study.

Due to problems of space, only a few of these matrices are explicitly listed in this paper. With some knowledge of group theory, the remaining matrices can be generated from the ones listed. A complete listing however, of these matrices and other details not available in this report have been provided elsewhere [9].

2. GROUP THEORY AND THE MOLECULAR ORBITALS

The structure of the C_{60} molecule has been determined explicitly through well known experiments. There are 12 pentagons and 20 hexagons in the C_{60} molecule, which correspond to those of a truncated icosahedron. The 120-element icosahedral point group of the C_{60} molecule, I_h, is the cross-product of the 60-element icosahedral rotation group I and the inversion group C_i, i.e. $I_h = I \otimes C_i$. The inversion group C_i contains only the unit operator and the inversion operator, both of which commute with the 60 proper rotations in I. Thus the elements of the full I_h are generated by first operating on all the elements of I with the unit operator of C_i, replicating the class structure of I; then all the elements of I are next multiplied with the inversion operator of C_i, creating 60 new improper rotations. Thus, the 120 point-group elements (R) of I_h contain 12 five fold axes (C_5) passing through the pentagon centers, 20 three fold axes (C_3) passing through the hexagon centers, 15 t wofold axes (C_2) passing through the midpoint of the hexagon-hexagon edges and a center of inversion (i). On the whole, I_h has 10 classes $\left(E, 12C_5, 12C_5^2, 20C_3, 15C_2, i, 12S_{10}, 12S_{10}^3, 20S_6, 15\sigma\right)$ and 10 irreducible representations. The characters $\chi^i(R)$ of the icosahedral group for the three irreducible representations $\left(t_{1g}, t_{1u}, h_u\right)$, relevant to this work are given in Table 1. The characters have been taken from Ref. 8.

In what follows, we shall view the C_{60} molecule as a ball-shaped lattice with one carbon atom at each lattice site. To investigate the electronic properties of a single C_{60} molecule, one normally starts with the four carbon valence electrons 2S, $2P_x$, $2P_y$ and $2P_z$ at each carbon atom site of the molecule. The 60 $2P_z$ orbitals, each pointing along the outward radial direction, are hybridized to form π states. The other three orbitals 2S, $2P_x$ and $2P_y$, distributed on the plane tangential to the surface of the molecule are hybridized along the lattice bonds to form σ bonding and antibonding states. While the 60 outer π orbitals are relevant to the conducting properties of the molecule and only π states occur around the fermi energy, the 180σ orbitals are mainly responsible for the elastic properties of the molecule. For solid C_{60}, the highest valence bands and the lowest conduction bands are derived, respectively from the fivefold degenerate highest occupied molecular orbital h_u(HOMO) and the threefold-degenerate lowest unoccupied molecular orbitals t_{1u}(LUMO) of the neutral C_{60} molecule. The bands t_{1g}, t_{1u} and h_u have primarily P_z (also called Pπ) character.

Table 1: Character $\chi^i(R)$ for three irreducible representations of the icosahedral group I_h

R	$\chi^i(R)$		
	$i = t_{1g}$	$i = t_{1u}$	$i = h_u$
E	3	3	5
$12C_5$	τ	τ	0
$12C_5^2$	$-\frac{1}{\tau}$	$-\frac{1}{\tau}$	0
$20C_3$	0	0	-1
$15C_2$	-1	-1	1
i	3	-3	-5
$12S_{10}$	$-\frac{1}{\tau}$	$\frac{1}{\tau}$	0
$12S_{10}^3$	τ	$-\tau$	0
$20S_6$	0	0	1
15σ	-1	1	-1

$$\tau = \tfrac{1}{2}\left(1+\sqrt{5}\right)$$

Since these are the bands that feature in the superconductivity of the doped C_{60} system, and since the phenomenon of superconductivity is one of our major motivations for studying the electronic structure of the C_{60} system, our usage of only the $2P_z$ orbital per carbon atom in the construction of the C_{60} molecular orbital (MO) is a reasonable starting point.

We show in Fig. 1 the C_{60} molecule with its atomic positions indicated. The coordinates of the 60 atomic positions, with respect to an origin at the center of the molecule, are fully listed in Appendix 1. As earlier stated this molecule has 120 symmetry elements (R) which are grouped into 10 classes. The 3 x 3 matrix representation $\hat{R}$ for each symmetry element R has been worked out and fully listed elsewhere [9]. We give in Appendix 2 a few of these matrices. Taking into account Fig. 1 and the listing in Appendix 1, the other matrices can be worked out from those already given.

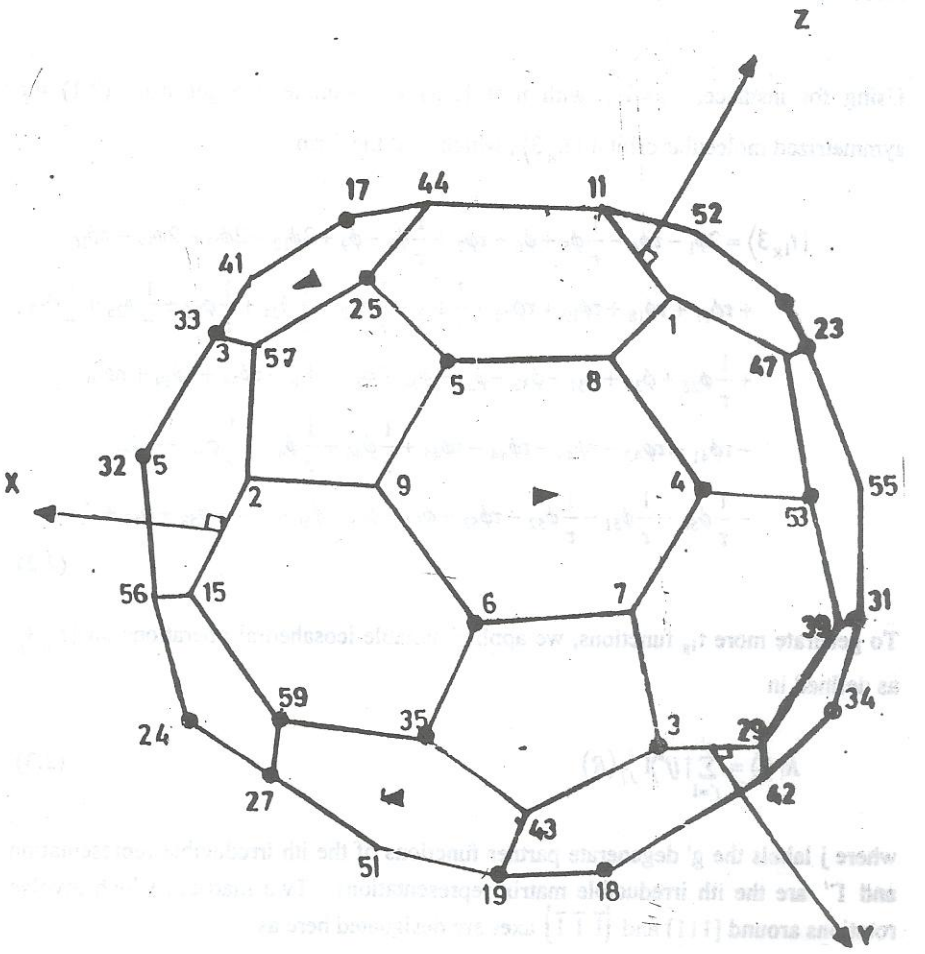

Fig 1. The C_{60} molecule in the y-orientation with atomic positions 1, 2, 3, . . . indicated. The co-ordinates of the atom positions with respect to an origin at the center of the molecule, are given in Appendix 1.

With the above tools at hand, we can now use the characters to project out of the carbon P_z orbital $|n\rangle$ or ϕ_n at atomic site n the part $|i\rangle$ which belongs to the ith irreducible representation, in the sense

$$|i\rangle = \sum_{R=1}^{120} \chi^i(R)\hat{R}|n\rangle \qquad (2.1)$$

Using for instance, $i = t_{1g}$ with n = 1, as an example, we get from (2.1) the symmetrized molecular orbital $|t_{1g}3\rangle$, which is of the form

$$|t_{1g}3\rangle = 2\phi_1 - \tau\phi_4 - \frac{1}{\tau}\phi_5 + \phi_6 + \tau\phi_7 + \frac{1}{\tau}\phi_8 - \phi_9 + 2\phi_{10} - 2\phi_{11} - 2\phi_{12} - \tau\phi_{16}$$
$$+ \tau\phi_{17} + \tau\phi_{18} + \tau\phi_{19} + \tau\phi_{20} - \frac{1}{\tau}\phi_{22} - \frac{1}{\tau}\phi_{23} - \frac{1}{\tau}\phi_{24} + \frac{1}{\tau}\phi_{25} + \frac{1}{\tau}\phi_{26} + \frac{1}{\tau}\phi_{27},$$
$$+ \frac{1}{\tau}\phi_{28} + \phi_{30} + \phi_{31} + \phi_{32} - \phi_{33} - \phi_{34} - \phi_{35} - \phi_{36} + \tau\phi_{38} + \tau\phi_{39} + \tau\phi_{40}$$
$$- \tau\phi_{41} - \tau\phi_{42} - \tau\phi_{43} - \tau\phi_{44} - \tau\phi_{45} + \frac{1}{\tau}\phi_{46} + \frac{1}{\tau}\phi_{47} + \frac{1}{\tau}\phi_{48} - \frac{1}{\tau}\phi_{49}$$
$$- \frac{1}{\tau}\phi_{50} - \frac{1}{\tau}\phi_{51} - \frac{1}{\tau}\phi_{52} - \tau\phi_{53} - \phi_{54} - \phi_{55} - \phi_{56} + \phi_{57} + \phi_{58} + \phi_{59} + \phi_{60} \qquad (2.2)$$

To generate more t_{1g} functions, we applied suitable icosahedral operations on $|t_{1g}3\rangle$ as defined in

$$R|ij\rangle = \sum_{j'=1}^{g^i} |ij'\rangle \Gamma^i_{j'j}(R) \qquad (2.3)$$

where j labels the g^i degenerate partner functions of the ith irreducible representation and Γ^i are the ith irreducible matrix representations. Two matrices which involve rotations around [111] and $[\bar{1}\,\bar{1}\,\bar{1}]$ axes are designated here as

$$\hat{R}_3 = \begin{bmatrix} 0 & 1 & 0 \\ 0 & 0 & 1 \\ 1 & 0 & 0 \end{bmatrix} \quad \text{and} \quad \hat{\bar{R}}_3 = \begin{bmatrix} 0 & 0 & 1 \\ 1 & 0 & 0 \\ 0 & 1 & 0 \end{bmatrix}$$

respectively. Turning $|t_{1g}3\rangle$ around [111] and $[\bar{1}\,\bar{1}\,\bar{1}]$ axes results in

$$|t_{1g}1\rangle = \hat{R}_3|t_{1g}3\rangle = 2\phi_3 - \frac{1}{\tau}\phi_4 + \phi_5 - \tau\phi_6 + \frac{1}{\tau}\phi_7 - \phi_8 + \tau\phi_9 + \frac{1}{\tau}\phi_{16} + \frac{1}{\tau}\phi_{17} + \frac{1}{\tau}\phi_{18}$$
$$- \frac{1}{\tau}\phi_{19} - \frac{1}{\tau}\phi_{20} + 2\phi_{21} + \phi_{22} - \phi_{23} - \phi_{24} - \phi_{25} - \phi_{26} + \phi_{27} + \phi_{28} - 2\phi_{29} - \tau\phi_{30}$$
$$+ \tau\phi_{31} + \tau\phi_{32} + \tau\phi_{33} + \tau\phi_{34} - \tau\phi_{35} - \tau\phi_{36} - 2\phi_{37} + \frac{1}{\tau}\phi_{38} - \frac{1}{\tau}\phi_{39} - \frac{1}{\tau}\phi_{40} \qquad (2.4)$$
$$- \frac{1}{\tau}\phi_{41} - \frac{1}{\tau}\phi_{42} + \frac{1}{\tau}\phi_{43} + \frac{1}{\tau}\phi_{44} - \frac{1}{\tau}\phi_{45} - \phi_{46} + \phi_{47} + \phi_{48} + \phi_{49} + \phi_{50}$$
$$- \phi_{51} - \phi_{52} + \frac{1}{\tau}\phi_{53} + \tau\phi_{54} - \tau\phi_{55} - \tau\phi_{56} - \tau\phi_{57} - \tau\phi_{58} + \tau\phi_{59} + \tau\phi_{60}$$

$$|t_{1g}2\rangle = \hat{\bar{R}}_3|t_{1g}3\rangle = 2\phi_2 + \phi_4 - \tau\phi_5 - \frac{1}{\tau}\phi_6 - \phi_7 + \tau\phi_8 + \frac{1}{\tau}\phi_9 + 2\phi_{13} - 2\phi_{14} - 2\phi_{15}$$
$$- \phi_{16} + \phi_{17} + \phi_{18} - \phi_{19} - \phi_{20} - \tau\phi_{22} + \tau\phi_{23} + \tau\phi_{24} - \tau\phi_{25} - \tau\phi_{26} + \tau\phi_{27} + \tau\phi_{28}$$
$$- \frac{1}{\tau}\phi_{30} + \frac{1}{\tau}\phi_{31} + \frac{1}{\tau}\phi_{32} - \frac{1}{\tau}\phi_{33} - \frac{1}{\tau}\phi_{34} + \frac{1}{\tau}\phi_{35} + \frac{1}{\tau}\phi_{36} - \phi_{38} + \phi_{39} + \phi_{40} - \phi_{41} \qquad (2.5)$$
$$- \phi_{42} + \phi_{43} + \phi_{44} + \phi_{45} + \tau\phi_{46} - \tau\phi_{47} - \tau\phi_{48} + \tau\phi_{49} + \tau\phi_{50} - \tau\phi_{51} - \tau\phi_{52} - \phi_{53}$$
$$+ \frac{1}{\tau}\phi_{54} - \frac{1}{\tau}\phi_{55} - \frac{1}{\tau}\phi_{56} + \frac{1}{\tau}\phi_{57} + \frac{1}{\tau}\tau\phi_{58} - \frac{1}{\tau}\phi_{59} - \frac{1}{\tau}\phi_{60}$$

$|t_{1g}1\rangle$, $|t_{1g}2\rangle$ and $|t_{1g}3\rangle$ are called partner functions for the t_{1g} irreducible representation. Three such functions are also required for the t_{1u} representation, while five are needed for the h_u representation. In view of the band structure calculation to be carried out in the next section, we may rewrite these functions more compactly as

$$|ij\rangle = \sum_{n=1}^{60} |n\rangle C_{nj}^{i} \qquad (2.6)$$

where i denotes the representation and j the partner function, while C_{nj}^{i} are of course the coefficients of the atomic orbitals ϕ_n in the expressions (2.2) or (2.4), etc.

The three t_{1g} functions are congruent and have $\chi(\sigma) = -1$, i.e. the t_{1g} MO's are even with respect to one coordinate and odd with respect to the remaining two coordinates. The labelling convention for the t_{1g} functions is as follows: $|t_{1g}K\rangle$ is even with respect to the coordinate K (K = 1,2,3). The t_{1g} level or band structure is the LUMO in alkali-doped solid C_{60}.

The t_{1u} representation is like the t_{1g} except that the t_{1u} representation is odd rather than even under inversion. The t_{1u} MO's are also congruent and related to each other through rotations around the [111] and $[\bar{1}\,\bar{1}\,\bar{1}]$ axes. Unlike the t_{1g}, the t_{1u} representation occurs twice in the space of the 60 AO's. This leads to the division of

the t_{1u} space into the MO's of the upper level, denoted with a *, and those of the lower level without a *. Thus, the t_{1u}^* level is the LUMO in pure solid C_{60} and it is partly occupied in alkali-doped solid C_{60}; and since the t_{1g} and t_{1u}^* bands are the levels that are relevant to superconductivity , they are the levels that are calculated in this work. The fivefold degenerate h_u level is the HOMO in pure solid C_{60}. Like the t_{1u}, the h_u representation also occurs twice in the space of the 60 AO's but for h_u, one is usually interested in the lowest h_u level. Much more details on these levels or bands, than contained here can be found in the literature [5 – 7, 12 – 16].

3 BAND STRUCTURES

(a) Atomic orbitals (AO's) and the hopping terms:

The tight-binding Hamiltonian is defined as [5]

$$H = \sum_{l,\mu} E_{l,\mu} c_{l,\mu}^{+} c_{l,\mu} + \sum_{<l,\mu;m,\nu>} V_{\mu,\nu}(r_{lm}) \left(c_{l,\mu}^{+} c_{m,\nu} + HC \right) \tag{3.1}$$

In Eq. (3.1), l and m label atomic sites while μ and v label atomic orbitals (S, P_x, P_y, P_z). The angular brackets <...> indicates a sum over all sites and is restricted to nearest neighbours. $c_{l,\mu}^{+}$ creates an electron in the orbital μ at site l while $c_{l,\mu}$ annihilates the electron at the same location. The on-site energy term is represented by $E_{l,\mu}$ while $V_{\mu,\nu}(r_{lm})$ are the hopping integrals. The hopping terms are designed to decay rapidly with interatomic distance r_{lm} and are also given in terms of the two-centre integrals written as $V_{ss\sigma}(r_{lm})$, $V_{sp\sigma}(r_{lm})$, $V_{pp\sigma}(r_{lm})$, and $V_{pp\pi}(r_{lm})$. The hopping integral between the P orbitals on different atoms l and m has the expression

$$< m \mid H \mid l >= -\{V_\sigma(d) - V_\pi(d)\}(\hat{R}_m \cdot \hat{d})(\hat{R}_l \cdot \hat{d}) + V_\pi(d)(\hat{R}_m \cdot \hat{R}_l) \tag{3.2}$$

Where $\hat{R}_l$ is a unit vector in the direction of the P orbital on atom l, $\hat{d}(= \mathbf{d}/d)$ is also a unit vector in the direction starting from atom m to atom l and 'd' is the distance between them. The relationship between $V_\sigma(d)$ and $V_\pi(d)$ is $V_\sigma(d) = -4V_\pi(d)$ as recommended by Harrison [10] while the distance-dependence is parametrized according to

$$V_\sigma(d) = V_0 \frac{d}{d_0} \exp\left(-\frac{d - d_0}{L} \right) \tag{3.3}$$

with L = 0.505 Å , V_0 = 0.90eV, and d_0 = 3.0 Å

The simplest structure with the C_{60} molecules on a fcc lattice is obtained if all molecules have the same orientation, thus leading to a structure with one molecule per primitive unit cell. Among the structures with one molecule per primitive cell, the one with the lowest energy seems to be the one where the local x, y and z axes, i.e., the molecular twofold axes, coincide with the x, y and z axes of the lattice. This structure has the space group $Fm\bar{3}$ and since it is the one normally considered in LDA calculations, it is the one also considered here. Two orientations are possible for this structure. If the double-bonded hexagon edge with the highest z coordinate in each C_{60} molecule is arranged to be perpendicular to the z-axis and parallel to the x-axis we obtain the so-called X-orientation [7]. But if the double-bonded hexagon edge with the highest z coordinate in each C_{60} molecule is made perpendicular to the z-axis and parallel to the y-axis we get the y-orientation which is adopted in this work and shown in Fig. 1.

We refer to the two structures just described as the unidirectional structure, since all molecules in the solid have the same orientation, x or y. For this structure in the y-orientation, the molecule-molecule contacts in the C_{60} solid consist of parallel single bonds, involving, for instance, atoms 6 and 35 on the molecule at the origin and atoms 36 and 30 on the nearest neighbour molecule at the fcc lattice site $\left(\frac{a}{2},\frac{a}{2},0\right)$. In general, the contact atoms in the positive octant for the molecule at the origin are the atoms numbered 4, 5 and 6. The contact atoms for the remaining 7 octants can be easily determined. These contacts atoms form the closest contact to the nearest neighbour molecules in the fcc lattice. With all the molecules "parallel", the intermolecular nearest-neighbour-atom distance and the corresponding AO hopping integral are, respectively, $d_{11} = 3.05\,\mathring{A}$ and $V_{11} = 742$meV for a lattice constant of a = $14.1\,\mathring{A}$.

(b) **LUMO sub-bands:**

Let the ket $|ijn\rangle$ represent the jth partner function of the ith representation MO at site n. In order to calculate the band structure for a crystal with lattice translations $\vec{T}$ and molecules at the N sites $\vec{t}$ (now inside the primitive cell), we construct Bloch sums

$$\left|ij\,\vec{t}\,\vec{K}\right\rangle = \sum_{\vec{T}} \left|ij,\vec{t}+\vec{T}\right\rangle \exp\left\{i\vec{K}\cdot\left(\vec{t}+\vec{T}\right)\right\} \tag{3.4}$$

of the MO's (2.6) at sites $\vec{t}+\vec{T}$ and then evaluate the matrix elements,

$$\left\langle ij'\vec{t}'\vec{K}\middle|H\middle|ij\vec{t}\,\vec{k}\right\rangle = \sum_{\vec{T}} exp\left\{i\vec{K}\cdot\left(\vec{t}-\vec{t}'+\vec{T}\right)\right\}\left\langle ij',\vec{t}'\middle|H\middle|ij,\vec{t}+\vec{T}\right\rangle \tag{3.5}$$

of the one-electron Hamiltonian between these Bloch sums.

The matrix elements on the right-hand side of (3.5) are the MO transfer integrals, and they are related to the AO transfer integrals $\langle n'|H|n\rangle$ through the equation,

$$\langle ij',\vec{t}'|H|ij,\vec{t}+\vec{T}\rangle = \sum_{n'n} C^{i}_{n'j'}\langle n'|H|n\rangle C^{i}_{nj} \qquad (3.6)$$

The integer n runs over the 60 atoms of the molecule centered at $\vec{t}+\vec{T}$ and n' runs over the atoms of the molecule centered at $\vec{t}'$.

Note that, in Eq. (3.5), the matrix elements between Bloch sums of different $\vec{k}$'s in the Brillouin zone vanish for a crystal, and those between MO's from different molecular levels i are neglected in the single-MO approach adopted here.

Taking into account section 3a above, the integral for hopping between the MO's $|ij',0\rangle$ and $|ij,\vec{t}\rangle$ on neighbouring molecules may now be easily calculated by summing over the AO's on the two molecules according to (3.6). Since the diameter D of the molecule is approximately 3τ which is approximately five times the bond length b, which itself is nearly three times the decay length L of the AO hopping in (3.3), the sums in (3.6) are effectively limited to a small region between the molecules, the so-called "contact region". Moreover, MO hoppings beyond nearest-neighbour molecules can safely be neglected.

Diagonalization of the 3 x 3 Hamiltonian matrix (3.5) yields the ith representation band structure $E^{i}_{\nu}\left(\vec{K}\right)$ where ν enumerates the sub-bands. The eigenvalues $E^{i}_{\nu}\left(\vec{K}\right)$ are easily calculated once the wave-vector $\vec{K}$ is specified.

We can simplify further Eq. (3.5) since only nearest neighbour molecules are involved in the summation. In this connection, let the 4 molecules in the XY plane that are nearest neighbours to the central molecule at the origin possess the position vectors $\vec{x}(l)$ with l = 1,2,3,4 and where $\vec{x}(1)=\frac{a}{2}(1,1,0)$, $\vec{x}(2)=\frac{a}{2}(-1,-1,0)$, $\vec{x}(3)=\frac{a}{2}(1,-1,0)$, and $\vec{x}(4)=\frac{a}{2}(-1,1,0)$. Then the matrices M describing the hopping terms from the central molecule to its 4 nearest neighbours may be written as

$$M(0,l)=\frac{1}{4}\begin{pmatrix} C_{xy} & S_{xy} & 0 \\ S_{xy} & E_{xy} & 0 \\ 0 & 0 & D_{xy} \end{pmatrix}, \qquad :l=1,2 \tag{3.7a}$$

and

$$M(0,l)=\frac{1}{4}\begin{pmatrix} C_{xy} & -S_{xy} & 0 \\ -S_{xy} & E_{xy} & 0 \\ 0 & 0 & D_{xy} \end{pmatrix} \qquad :l=3,4 \tag{3.7b}$$

Similarly, hopping to the 4 neighbours on the XZ plane may be written in matrix form as

$$M(0,l)=\frac{1}{4}\begin{pmatrix} E_{xz} & 0 & S_{xz} \\ 0 & D_{xz} & 0 \\ S_{xz} & 0 & C_{xz} \end{pmatrix} \qquad :l=5,6 \tag{3.7c}$$

and

$$M(0,l)=\frac{1}{4}\begin{pmatrix} E_{xz} & 0 & -S_{xz} \\ 0 & D_{xz} & 0 \\ -S_{xz} & 0 & C_{xz} \end{pmatrix} \qquad :l=7,8 \tag{3.7d}$$

where the 4 molecules denoted by l = 5,6,7 and 8 possess the position vectors $\vec{x}(5)=\frac{a}{2}(1,0,1)$, $\vec{x}(6)=\frac{a}{2}(-1,0,-1)$, $\vec{x}(7)=\frac{a}{2}(1,0,-1)$, and $\vec{x}(8)=\frac{a}{2}(-1,0,1)$. Finally, hopping from the central molecule to its 4 neighbours on the yz planes takes the form

$$M(0,l)=\frac{1}{4}\begin{pmatrix} D_{yz} & 0 & 0 \\ 0 & C_{yz} & S_{yz} \\ 0 & S_{yz} & E_{yz} \end{pmatrix} \qquad :l=9,10 \tag{3.7e}$$

and

$$M(0,l)=\frac{1}{4}\begin{pmatrix} D_{yz} & 0 & 0 \\ 0 & C_{yz} & -S_{yz} \\ 0 & -S_{yz} & E_{yz} \end{pmatrix} \qquad :l=11,12 \tag{3.7f}$$

where the 4 neighbour molecules possess the position vectors

$\vec{x}(9)=\frac{a}{2}(0,1,1)$, $\vec{x}(10)=\frac{a}{2}(0,-1,-1)$, $\vec{x}(11)=\frac{a}{2}(0,1,-1)$, and $\vec{x}(12)=\frac{a}{2}(0,-1,1)$.

These matrices must fulfil certain selection rules or symmetry requirements. In particular,

$$\left.\begin{aligned} E_{xy} &= E_{xz} = E_{yz} \\ C_{xy} &= C_{xz} = C_{yz} \\ S_{xy} &= S_{xz} = S_{yz} \\ \text{and } D_{xy} &= D_{xz} = D_{yz} \end{aligned}\right\} \tag{3.8}$$

In terms of these matrices, the tight-binding (nearest neighbours only) Hamiltonian matrix (3.5) now take the form

$$H_{\alpha\beta}\left(\vec{K}\right) = \sum_{l=1}^{12} M_{\alpha\beta}(0,l)\exp\left\{i\vec{K}\cdot\vec{x}(l)\right\} \tag{3.9}$$

with $\alpha, \beta = 1,2,3$

Eqn. (3.9) can be easily worked out to give

$$H_{11}\left(\vec{K}\right) = C_{xy}\cos\left(\frac{ak_x}{2}\right)\cos\left(\frac{ak_y}{2}\right) + E_{xz}\cos\left(\frac{ak_x}{2}\right)\cos\left(\frac{ak_z}{2}\right) + D_{yz}\cos\left(\frac{ak_y}{2}\right)\cos\left(\frac{ak_z}{2}\right)$$

$$H_{22}\left(\vec{K}\right) = E_{xy}\cos\left(\frac{ak_x}{2}\right)\cos\left(\frac{ak_y}{2}\right) + C_{yz}\cos\left(\frac{ak_y}{2}\right)\cos\left(\frac{ak_z}{2}\right) + D_{xz}\cos\left(\frac{ak_z}{2}\right)\cos\left(\frac{ak_x}{2}\right)$$

$$H_{33}\left(\vec{K}\right) = C_{xz}\cos\left(\frac{ak_z}{2}\right)\cos\left(\frac{ak_x}{2}\right) + E_{yz}\cos\left(\frac{ak_y}{2}\right)\cos\left(\frac{ak_z}{2}\right) + D_{xy}\cos\left(\frac{ak_x}{2}\right)\cos\left(\frac{ak_y}{2}\right)$$

$$H_{12}\left(\vec{K}\right) = H_{21}\left(\vec{K}\right) = S_{xy}\sin\left(\frac{ak_x}{2}\right)\sin\left(\frac{ak_y}{2}\right) \tag{3.10}$$

$$H_{13}\left(\vec{K}\right) = H_{31}\left(\vec{K}\right) = S_{xz}\sin\left(\frac{ak_x}{2}\right)\sin\left(\frac{ak_z}{2}\right)$$

$$H_{23}\left(\vec{K}\right) = H_{32}\left(\vec{K}\right) = S_{yz}\sin\left(\frac{ak_y}{2}\right)\sin\left(\frac{ak_z}{2}\right)$$

The expressions (3.10) agree with the Hamiltonian matrix elements given in Ref 7 if account is taken of the change in notation. The coefficients

C_{xy}, E_{yz}, and D_{xz} in this work are the coefficients labeled, respectively, $\langle 1|C_{xy}|1\rangle$, $\langle 3|C_{yz}|3\rangle$, and $\langle 2|C_{zx}|2\rangle$ in Ref 7. Eq. (3.8) implies that there are only 4 independent coefficients in (3.10). These independent coefficients can be determined by fitting to accurately calculated band structures or by using (3.6) together with (3.2) and (3.3). The values of these coefficients in this work for the t_{1u}^{*} bands are

$$C_{xy} = 140.8meV\ ,\ E_{xy} = 65.44meV\ ,\ D_{xy} = -91.27meV \text{ and } S_{xy} = 96meV\ .$$

For the t_{1g} bands we have

$$C_{xy} = 28.26meV\ ,\ E_{xy} = 74.46meV\ ,\ D_{xy} = -194.47meV \text{ and } S_{xy} = 46meV$$

The Hamiltonian matrix simplifies tremendously for the Bloch vector $\vec{k}$ at lines and points of high symmetry. For instance, at the high symmetry point L where $\vec{k} = (1,1,1)\frac{\pi}{a}$, we get for the t_{1u}^{*} representation the Hamiltonian matrix,

$$H = \begin{pmatrix} 0 & S_{xy} & S_{xz} \\ S_{xy} & 0 & S_{yz} \\ S_{xz} & S_{yz} & 0 \end{pmatrix} \tag{3.11}$$

with the eigenvalues

$$^{1}E_{L} = {}^{2}E_{L} = -S_{xy} = -96meV$$

and

$$^{3}E_{L} = 2S_{xy} = 192meV$$

The results obtained for the t_{1u}^{*} representation band structure are plotted in Fig.3 for the various symmetry directions, while that for the t_{1g} are plotted in Fig.2.

The corresponding density of states (DOS) is calculated from the usual definition

$$N(E) \propto \iint \frac{ds}{|grad\ E|} \tag{3.12}$$

which is an integration over the surface in k-space for which the energy has a constant value E. The calculation of the DOS was performed with 2 special k points [11] and smoothened by convoluting the energy spectrum with a gaussian of width W(E), the band-width. The results got are displayed in Fig.4 for the t_{1u}^{*} bands.

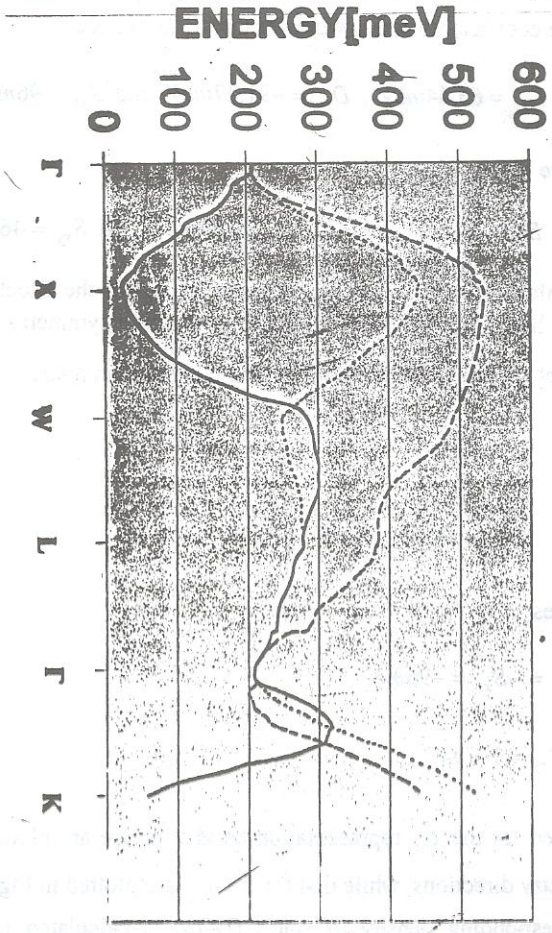

Fig. 2 t_{1g} bands for a = 14.10 A^{0}

Fig. 2 t_{1g} bands for a = 14.10 A

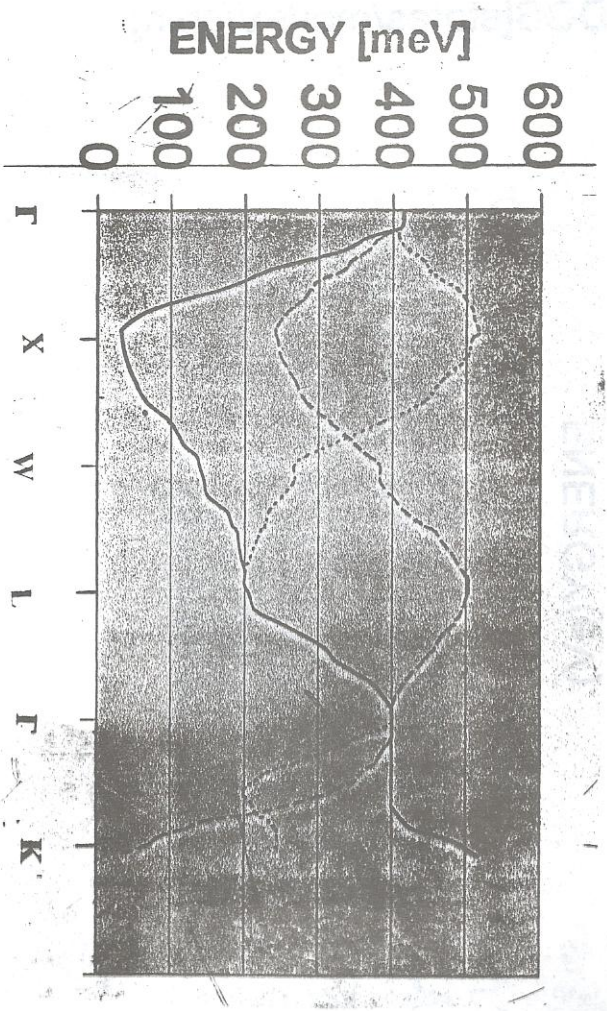

Fig 3 t_{1u}^{*} bands for a = 14.10 $\mathring{A}$

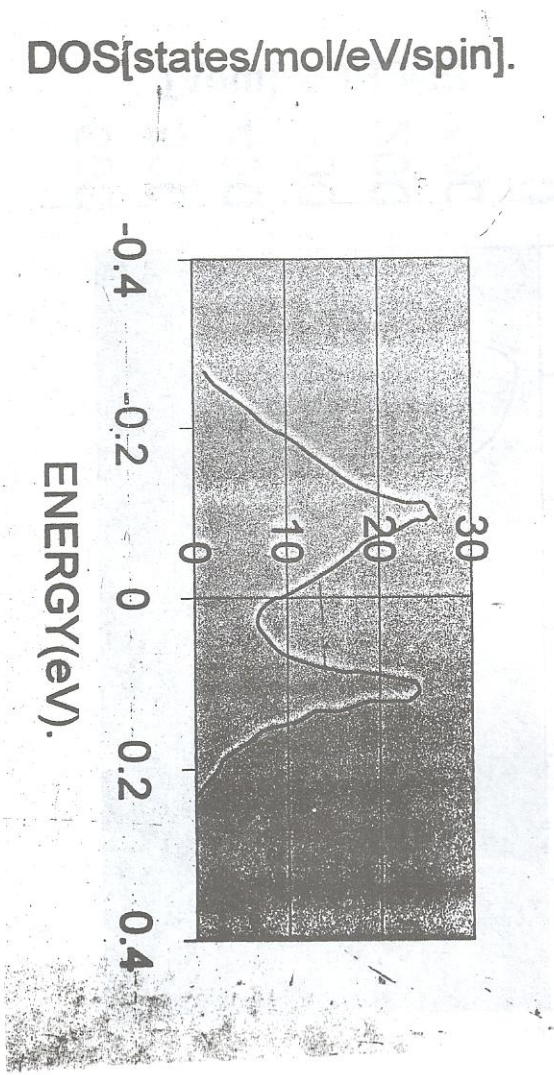

Fig. 4 :Density of states of solid C_{60}.

Fig 4: Density of staters of solid C_{60}

Table 2. t_{1u}^{*} band-width W(E)

	a	b	c	d	e	f	g
W(E) in (eV)	0.447	0.504	0.552	0.701	0.749	0.430	0.420

a Present work
b Linear combination of Atomic orbitals (LCAO) [12]
c Plane Wave Pseudo-potential (PW) [13]
d L C A O [14]
e Linear-Muffin-Tin Orbitals (LMTO-FP) [15]
f Local Density Approximation (LDA) [16]
g Local Density Approximation (LDA) [5]

4 RESULTS AND DISCUSSION

The derivation of the 120 matrix representations for the 120 symmetry elements of the C_{60} molecule enabled us to construct fully symmetrized molecular orbitals (MO's). These transform among each other under the covering operations (R) of the C_{60} molecule according to the irreducible representations of the icosahedral group.

The formation of the Bloch sums for the MO's at sites $\vec{n}+\vec{T}$ in the crystal allowed the evaluation of the matrix elements of the single-particle tight-binding Hamiltonian. This led to the calculation of the t_{1g} and t_{1u}^{*} band structures plotted in Figs 2 and 3 respectively. Their energy minimum is clearly located at the X point. The value recorded by us for the conduction band-width of the pure solid C_{60} is 0.447eV which agrees with experiments and other calculations, as shown in Table 2.

The fundamental assumption of the tight-binding approximation as applicable to solid C_{60} is that the molecules be fart apart enough for the interaction between them to be small. This weak interaction is responsible for the broadening of the isolated energy levels of the C_{60} molecule into bands of allowed energies in the crystalline solid. It follows on the ground of consistency, that the widths obtained must be comparatively small. Our band-width satisfies this criterion. The advantage of our method is in its simplicity. A problem that would have required matrices as large as 60 x 60, was reduced, with the aid of group theory, to matrixes of size 3 x 3.

The density of states computed by us over the range of energy values $\pm$0.3eV is also displayed in Fig 4 for solid C_{60}.

5. CONCLUSION

As indicated in the introductory part, the application of group theory to the C_{60} molecule immensely simplified the task of calculating the electronic band structures of the pure solid. Our approach, apart from providing the group theoretical

data on the C_{60} molecule (and of course solid C_{60}), also provide a proper theoretical procedure for understanding the composition and structure if the alkali-metal doped solid C_{60}. The band structure of the alkali-metal doped C_{60} and its implications for superconductivity are discussed in the following paper [17].

One can proceed to make further investigations and to extend the analytical calculations to bi-directional structural order which most probably is the actual orientational structural order for the superconducting phase of these materials. In this case, the model tight-binding Hamiltonian matrix elements will be 6-dimensional (i.e. N = 2)

Appendix 1: Coordinates of the 60 atoms of the C_{60} molecule in the y-orientation in units of b/2 where b is the bond length. [For realistic calculations, allowance must be made for the fact that single bonds are of length $(1 + \epsilon)$b while double bonds are of length $(1 - 2\epsilon)$b. For pure C_{60}, $\epsilon \approx 0.015$ and it is a measure of the bond alternation].

1) (0, 1, 3τ)	21) (-1, -3τ, 0)	41) (2, -2τ-1, τ)
2) (3τ, 0, 1)	22) (-2τ, -1, -2-τ)	42) (-2, 2τ+1, -τ)
3) (1, 3τ, 0)	23) (-2τ, +1, 2+τ)	43) (2, 2τ+1, -τ)
4) (1, 2+τ, 2τ)	24) (2τ, -1, -2-τ)	44) (-2, -2τ-1, τ)
5) (2τ, 1, 2+τ)	25) (2τ, -1, 2+τ)	45) (-1, -2-τ, -2τ)
6) (2+τ, 2τ, 1)	26) (-2τ, 1, -2-τ)	46) (-τ, -2, -2τ-1)
7) (2, 2τ+1, τ)	27) (2τ, 1, -2-τ)	47) (-τ, 2, 2τ+1)
8) (τ, 2, 2τ+1)	28) (-2τ, -1, 2+τ)	48) (τ, -2, -2τ-1)
9) (2τ+1, τ, 2)	29) (-1, 3τ, 0)	49) (τ, -2, 2τ+1)
10) (0, -1, -3τ)	30) (-2-τ, -2τ, -1)	50) (-τ, 2, -2τ-1)
11) (0, -1,3τ)	31) (-2-τ, 2τ, 1)	51) (τ, 2, -2τ-1)
12) (0, 1, -3τ)	32) (2+τ, -2τ, -1)	52) (-τ, -2, 2τ+1)
13) (-3τ, 0, -1)	33) (2+τ, -2τ, 1)	53) (-1, 2+τ,,2τ)
14) (-3τ, 0, 1)	34) (-2-τ, 2τ, -1)	54) (-2τ-1, -τ, -2)
15) (3τ, 0, -1)	35) (2+τ, 2τ, -1)	55) (-2τ-1, τ, 2)
16) (1, -2-τ, -2τ)	36) (-2-τ, -2τ, 1)	56) (2τ+1, -τ, -2)
17) (1, -2-τ, 2τ)	37) (1, -3τ,0)	57) (2τ+1, -τ, 2)
18) (-1, 2+τ, -2τ)	38) (-2, -2τ-1, -τ)	58) (-2τ-1, τ, -2)
19) (1, 2+τ, -2τ)	39) (-2, 2τ+1, τ)	59) (2τ+1, τ, -2)
20) (-1, -2-τ, 2τ)	40) (2, -2τ-1, -τ)	60) (-2τ-1, -τ, 2)

Appendix 2. Matrix representation $\hat{R}$ for each symmetry element R of the C_{60} molecule. With the exception of the single element classes, three matrices are listed below for each class. The rest can be worked out from those listed.

Class	Matrices		
E	$\begin{pmatrix} 1 & 0 & 0 \\ 0 & 1 & 0 \\ 0 & 0 & 1 \end{pmatrix}$		
$12C_5$	$\begin{pmatrix} \frac{\tau}{2} & -\frac{1}{2} & -\frac{1}{2\tau} \\ \frac{1}{2} & \frac{1}{2\tau} & \frac{\tau}{2} \\ -\frac{1}{2\tau} & -\frac{\tau}{2} & \frac{1}{2} \end{pmatrix}$	$\begin{pmatrix} \frac{1}{2} & \frac{1}{2\tau} & -\frac{\tau}{2} \\ \frac{1}{2\tau} & \frac{\tau}{2} & \frac{1}{2} \\ \frac{\tau}{2} & -\frac{1}{2} & \frac{1}{2\tau} \end{pmatrix}$	$\begin{pmatrix} \frac{1}{2\tau} & \frac{\tau}{2} & -\frac{1}{2} \\ -\frac{\tau}{2} & \frac{1}{2} & \frac{1}{2\tau} \\ \frac{1}{2} & \frac{1}{2\tau} & \frac{\tau}{2} \end{pmatrix}$
$12C_5^2$	$\begin{pmatrix} -\frac{1}{2\tau} & -\frac{\tau}{2} & -\frac{1}{2} \\ -\frac{\tau}{2} & \frac{1}{2} & -\frac{1}{2\tau} \\ \frac{1}{2} & \frac{1}{2\tau} & -\frac{\tau}{2} \end{pmatrix}$	$\begin{pmatrix} \frac{1}{2} & \frac{1}{2\tau} & \frac{\tau}{2} \\ -\frac{1}{2\tau} & -\frac{\tau}{2} & \frac{1}{2} \\ \frac{\tau}{2} & -\frac{1}{2} & -\frac{1}{2\tau} \end{pmatrix}$	$\begin{pmatrix} -\frac{\tau}{2} & \frac{1}{2} & \frac{1}{2\tau} \\ -\frac{1}{2} & -\frac{1}{2\tau} & -\frac{\tau}{2} \\ -\frac{1}{2\tau} & -\frac{\tau}{2} & \frac{1}{2} \end{pmatrix}$
$20C_3$	$\begin{pmatrix} -\frac{1}{2\tau} & \frac{\tau}{2} & -\frac{1}{2} \\ -\frac{\tau}{2} & -\frac{1}{2} & -\frac{1}{2\tau} \\ -\frac{1}{2} & \frac{1}{2\tau} & \frac{\tau}{2} \end{pmatrix}$	$\begin{pmatrix} 0 & 0 & 1 \\ -1 & 0 & 0 \\ 0 & -1 & 0 \end{pmatrix}$	$\begin{pmatrix} \frac{\tau}{2} & -\frac{1}{2} & \\ -\frac{1}{2} & -\frac{1}{2\tau} & \\ -\frac{1}{2\tau} & -\frac{\tau}{2} & \end{pmatrix}$
$15C_2$	$\begin{pmatrix} -\frac{\tau}{2} & -\frac{1}{2} & \frac{1}{2\tau} \\ -\frac{1}{2} & \frac{1}{2\tau} & -\frac{\tau}{2} \\ \frac{1}{2\tau} & -\frac{\tau}{2} & -\frac{1}{2} \end{pmatrix}$	$\begin{pmatrix} \frac{1}{2\tau} & -\frac{\tau}{2} & \frac{1}{2} \\ -\frac{\tau}{2} & -\frac{1}{2} & -\frac{1}{2\tau} \\ \frac{1}{2} & -\frac{1}{2\tau} & -\frac{\tau}{2} \end{pmatrix}$	$\begin{pmatrix} -1 & 0 & \\ 0 & 1 & \\ 0 & 0 & -1 \end{pmatrix}$
i	$\begin{pmatrix} -1 & 0 & 0 \\ 0 & -1 & 0 \\ 0 & 0 & -1 \end{pmatrix}$		
$12S_{10}$	$\begin{pmatrix} -\frac{1}{2} & -\frac{1}{2\tau} & \frac{\tau}{2} \\ \frac{1}{2\tau} & \frac{\tau}{2} & \frac{1}{2} \\ \frac{\tau}{2} & -\frac{1}{2} & \frac{1}{2\tau} \end{pmatrix}$	$\begin{pmatrix} \frac{1}{2\tau} & -\frac{\tau}{2} & -\frac{1}{2} \\ -\frac{\tau}{2} & -\frac{1}{2} & \frac{1}{2\tau} \\ \frac{1}{2} & -\frac{1}{2\tau} & \frac{\tau}{2} \end{pmatrix}$	$\begin{pmatrix} \frac{\tau}{2} & -\frac{1}{2} & \\ \frac{1}{2} & \frac{1}{2\tau} & \\ -\frac{1}{2\tau} & -\frac{\tau}{2} & \end{pmatrix}$
$12S_{10}^3$	$\begin{pmatrix} -\frac{1}{2} & \frac{1}{2\tau} & -\frac{\tau}{2} \\ \frac{1}{2\tau} & -\frac{\tau}{2} & -\frac{1}{2} \\ \frac{\tau}{2} & \frac{1}{2} & -\frac{1}{2\tau} \end{pmatrix}$	$\begin{pmatrix} -\frac{\tau}{2} & \frac{1}{2} & -\frac{1}{2\tau} \\ -\frac{1}{2} & -\frac{1}{2\tau} & \frac{\tau}{2} \\ -\frac{1}{2\tau} & -\frac{\tau}{2} & -\frac{1}{2} \end{pmatrix}$	$\begin{pmatrix} -\frac{1}{2} & \frac{\tau}{2} & \\ -\frac{\tau}{2} & -\frac{1}{2} & \\ -\frac{1}{2} & \frac{1}{2\tau} & \end{pmatrix}$

Class	Matrices		
$20S_6$	$\begin{pmatrix} \frac{1}{2\tau} & \frac{\tau}{2} & -\frac{1}{2} \\ -\frac{\tau}{2} & \frac{1}{2} & \frac{1}{2\tau} \\ -\frac{1}{2} & -\frac{1}{2\tau} & -\frac{\tau}{2} \end{pmatrix}$	$\begin{pmatrix} 0 & 1 & 0 \\ 0 & 0 & 1 \\ -1 & 0 & 0 \end{pmatrix}$	$\begin{pmatrix} \frac{1}{2} & -\frac{1}{2\tau} & -\frac{\tau}{2} \\ \frac{1}{2\tau} & -\frac{\tau}{2} & \frac{1}{2} \\ \frac{\tau}{2} & \frac{1}{2} & \frac{1}{2\tau} \end{pmatrix}$
15σ	$\begin{pmatrix} \frac{\tau}{2} & \frac{1}{2} & -\frac{1}{2\tau} \\ \frac{1}{2} & -\frac{1}{2\tau} & \frac{\tau}{2} \\ -\frac{1}{2\tau} & \frac{\tau}{2} & \frac{1}{2} \end{pmatrix}$	$\begin{pmatrix} -\frac{1}{2\tau} & \frac{\tau}{2} & -\frac{1}{2} \\ \frac{\tau}{2} & \frac{1}{2} & \frac{1}{2\tau} \\ -\frac{1}{2} & \frac{1}{2\tau} & \frac{\tau}{2} \end{pmatrix}$	$\begin{pmatrix} -1 & 0 & 0 \\ 0 & 1 & 0 \\ 0 & 0 & 1 \end{pmatrix}$

Note that the elements in each class possess the same trace or character as required by group theory.

REFERENCES

[1]. Kroto H.W., Heath J.R., O'Brien S.C., Curl R.F. and Smalley R.E. (1985), Nature (London) 318, 162.

[2]. Hebard A.F. (1992), Phys. Today 45, 26.

[3]. Fleming R.M. et al. (1991), Res. Soc. Symp. 206, 691.

[4]. Stephens P.W et al. (1991), Nature 351, 632.

[5]. Nacir Tit and Kumar Vijay (1993), J. Phys. Condens. Matter 9, 11151.

[6]. Lin Y-L and Nori F. (1996), Phys. Rev. B53, 1641.

[7]. Laouini N, Anderson O.K. and Gunnarson O. (1995) Phys. Rev B51, 16446.

[8]. Cotton F.A. (1963), Chemical Applications of Group Theory (New York: Wiley-Interscience, 2nd edition) ch. 7

[9]. Matthew-Ojelabi F., Ph.D Thesis (University of Benin, 2001)

[10]. Harrison W.A. (1989) Electronic Structure and Properties of Solids (New York: Dover) P. 149.

[11]. Chadi D.J. and Cohen M.L. (1973), Phys Rev. B8, 5747.

[12]. Xu Y.-N, Huang M. –Z and Ching W.Y. (1992), Phys Rev. B44, 13171 and Phys Rev. B 46, 4241.

[13]. Troullier N and Martins J.L. (1992), Phys Rev. B46, 1754.

[14]. Erwin S.C. and Pickett W.E. (1991), Science 254, 842.

[15]. Antropov V.P., Gunnarson A. and Liechtensein A.I. (1993), Phys. Rev. B 48, 7651.

[16]. Satpathy S., Antropov V.P., Andersen O.K., Jepsen O., Gunnarson O. and Leichtensein A.I. (1992). Phys. Rev. B 46, 1773.

[17]. Matthew-Ojelabi, F and Idiodi, J. O. A. (2001), J. Nig. Ass. Math. Phys. Vol. 5, 221